Magazine of Civil Engineering

ISSN 2712-8172

journal homepage: http://engstroy.spbstu.ru/

Research article

UDC 69

DOI: 10.34910/MCE.139.3

Behavior of white wood at elevated temperatures: insights from numerical and experimental studies

N. Otmani-Benmehidi[1] ✉ , ***M. Boudjadja***[1] , ***A. Otmani***[2]

[1] *Materials, Geomaterials and Environment Laboratory, Faculty of Technology, Badji Mokhtar Annaba University, Annaba, Algeria*

[2] *National Higher School of Technology and Engineering, Department of Process and Energy Engineering, Annaba, Algeria*

✉ *nadia.otmani@univ-annaba.dz*

Keywords: wood, specimen, high temperature, oven, properties, white wood, SAFIR

Abstract. This study investigates the fire behavior of white wood, a commercially dominant softwood in Algerian construction (cf. *Picea abies*). Using a combined experimental and numerical approach, the thermo-mechanical degradation of 8×8×32 cm specimens was analyzed. Experiments involved heating samples in an electric oven at 200 °C and 300 °C, with complementary simulations performed using the SAFIR software. The results confirm that elevated temperatures induce significant mass loss and a pronounced thermal gradient, with the core lagging behind the surface. This thermal degradation directly compromises mechanical properties, notably stiffness. Furthermore, the study establishes a clear link between physical phenomena – charring, smoke emission, mass loss – and the underlying degradation mechanisms. A critical finding was the failure of adhesive bonds at high temperatures, revealing a key vulnerability in assembled wooden structures under fire conditions. These findings provide essential data for modeling the fire performance of a vital local material, thereby informing safer regional construction practices.

Acknowledgements: We sincerely thank the laboratory managers at Annaba Higher School of Industrial Technologies for granting us access to the furnaces for our tests. We also extend our gratitude to Professor J-M. Franssen for providing the 2022 SAFIR software.

Citation: Otmani-Benmehidi, N., Boudjadja, M., Otmani, A. Behavior of white wood at elevated temperatures: insights from numerical and experimental studies. Magazine of Civil Engineering. 2025. 18(7). Article no. 13903. DOI: 10.34910/MCE.139.3

1. Introduction

Wood, a noble material used in construction for millennia, saw a decline in popularity following several major fires and the rise of steel, concrete, and the industrial revolution. Today, however, its unique ecological and aesthetic properties, along with its natural texture, are garnering renewed interest in the era of global environmental consciousness, sustainable development, and the pursuit of a harmonious society. Wood's exceptional natural and environmental performance is capturing attention once more. Notably, the production of concrete and steel is unsustainable and significantly harms our planet [1]. Historically, timber exploitation was challenging due to the difficulty of treating, cutting, and transporting wood. Yet, advances in machinery and factory processes have made these tasks much simpler and more efficient. Growing and harvesting wood has now become a beneficial method, with increasing advantages as large-scale construction with this material expands. Additionally, older trees absorb less CO_2 and produce less oxygen, making it more practical to harvest them and plant new ones in their place [2].

Therefore, the object of this study is to investigate the potential of white wood as a sustainable construction material, particularly in light of its historical use, ecological benefits, and current relevance amid global environmental awareness.

Timber is one of the three primary structural materials used in the construction of large structures, alongside steel and reinforced concrete. When utilized in building types where it is most structurally efficient, harvested timber can significantly reduce the environmental impact of construction [3–6]. Timber's strength parallel to grain is comparable to reinforced concrete: hardwood is slightly stronger, and softwood slightly weaker, although timber cannot match modern high-strength concrete in compression. While timber is less stiff than concrete and both materials are less stiff and strong than steel, timber's low density offers an advantage. This makes it particularly efficient for long-span or tall structures, where a significant portion of the load comes from the structure's own weight [6–9, 13].

Among the many advantages of timber, one of the most significant is that wood is one of the few building materials capable of storing carbon throughout the life of a building [10]. This storage capability helps reduce the carbon emissions released by trees at the end of their life cycle and mitigates the presence of other atmospheric carbon sources. It is generally estimated that 1 m^3 of wood can sequester 1 t of CO_2. Additionally, wood is the only building material sourced from renewable and sustainably managed resources: trees. Unlike materials that originate from non-renewable resources, wood is harvested from forests, making it an eco-responsible and sustainable choice [10, 11].

Wood is often defined as the secondary xylem in the stems of trees, consisting almost entirely of cell wall material. The properties of wood derive from its cell wall structures and the composition of wood polymers [12].

The main hemicelluloses of softwood are galactoglucomannan and arabinoglucuronoxylan, while in hardwood it is glucuronoxylan. Galactoglucomannan from softwood and glucuronoxylan from hardwood are decorated with acetyl groups (Fig. 1). Although it is unknown how different hemicelluloses impart properties to the cell walls, hemicelluloses are proposed to crosslink with cellulose by hydrogen bonds, which may influence the ability of the microfibrils to slip past one another [6]. Wood cell walls (fibers, tracheids, etc.) may be impregnated with lignin, making these walls impervious to water.

Lignin is also often regarded as the cementing agent that provides the cell wall rigidity and compressive strength. Extractives are a collective term for a series of organic compounds present in certain timbers in relatively small amounts, which include coloring matter, phenolics, turpentine, fatty acids, resin, and simple metabolic intermediates. Extractives impart colouration to the wood and give it its natural durability, as most of these compounds are toxic to both fungi and insects [6, 12].

In the secondary cell wall layers, the microfibrils are closely packed and parallel to each other. In addition to the cell lumen, the secondary cell wall is subdivided into three layers: S1, S2, and S3. Wood is highly anisotropic, meaning that its physical properties differ along different axes. The angle between the cellulose microfibrils and the longitudinal cell axis, the microfibril angle, is found to be a critical factor in determining the structural and mechanical properties. The varying fibril orientation in the particular layers (50°–70° in S1, 5–15° in S2, and 60–90° in S3) causes a mechanical locking effect, leading to a very high stiffness of the overall cell [4–6, 12]. Due to its thickness (90 % of the secondary cell wall) and low value of micro fibril angle, the S2 layer is responsible for the high tensile strength and stiffness and low shrinkage of wood in the longitudinal direction. Increased microfibril angle in the S2 layer decreases cell wall tensile strength and stiffness but increases the durability [10–13].

To answer the question why tomorrow's buildings should be made of timber, many studies on wood structures subject to fire have been carried out [14–38].

Hu et al. [15] conducted experimental studies and numerical simulations to investigate the mechanism of the incipient and growth stages of a building fire. The building, constructed in the 1980s with wooden components, has one compartment and one opening. The average fire load density was 1495.3 MJ/m^2, including the wooden columns, beams, furniture, etc. The evolution of indoor temperature, gas concentration, gas flow rate, and burning behaviors were obtained and analyzed in their work. This study helps to learn the characteristics of early and growth stages of building fires with wooden components.

Buchanan [16] has a review paper of the performance of timber buildings exposed to fire. Important distinctions are made between the impacts of pre- and post- flashover fires, and between the performance of light timber framing and heavy timber construction. Recent literature is reviewed.

Dietenberger [17] carried out work on the fire resistance of wood structures, using the ABAQUS software, through simulation, the temperature evolution can be observed in detail in the section and throughout the fire exposure.

Fawaz [18] and Park studied the thermal decomposition of wood. Park & Atreya [19] use 25.4 mm diameter dry wood spheres, both experimentally and theoretically. Pyrolysis of the wood spheres was conducted in a vertical tube furnace at temperatures ranging from 638 K to 879 K. During the pyrolysis process, mass loss and sample temperatures were measured. Center temperature measurements revealed two distinct thermal events, indicating sequential endothermic and exothermic reactions. A numerical study of these reactions, employing various pyrolysis kinetics models, was performed to elucidate the pyrolysis mechanism and the heats of the reactions. The comparison between experimental and numerical results showed that: (1) contrary to suggestions in the literature, the contributions of secondary tar decomposition and lignin decomposition to the center temperature exothermic peak are minimal; (2) the exothermic decomposition of the intermediate solid is responsible for the center temperature peak; (3) the center temperature plateau is due to the endothermic decomposition of cellulose; (4) internal pressure generation is critical as it controls the pyrolyzate mass transfer, thereby affecting both heat transfer and the residence time of the pyrolysis gases for secondary decomposition.

Gernay et al. [20] conducted an experimental study on timber columns, finding that they had a measured fire resistance of 55–58 min (for two specimens). However, when exposed to heating for 15 min, these columns failed during the cooling phase after 98–153 min (for two specimens).

Renard et al. [21] present the findings from six fire tests performed on glue laminated timber columns in a custom-built compartment. Wood cribs are used as fuel. The columns, 3680 mm long with a 280× ×280 mm^2 section, are subjected to constant axial loading during the whole fire duration. Column failure was observed in the six tests, with failure times ranging from 35 min to 71 min.

Elshayeb et al. [22] introduced an advanced methodology using the finite element method (FEM) to analyze square and circular wood columns by developing a virtual temperature history model. A numerical simulation model for the wood column was created using a two-dimensional mathematical framework based on Galerkin's Weighted Residual technique. This model focuses on the regional material properties of the wood column to describe its thermal behavior. By understanding the temperature history within a column and the relevant material properties, the column's strength can be calculated at any point during a fire.

Šulc et al. [23] introduce a heat transport model that incorporates a moving boundary condition, a criterion for finite element deactivation, and an internal heat source. Experimental comparisons using a constant radiative load show that the moving boundary condition becomes significant after approximately 10 min of fire exposure, leading to a consistent charring rate observed in multiple experiments.

Wichman & Atreya [24] developed a simplified model for the pyrolysis of charring materials, excluding the effects of moisture and assuming zero heat of pyrolysis. They identified four stages of pyrolysis: (i) inert heating, (ii) initial pyrolysis, (iii) thin char formation, and (iv) thick char formation. Formulas for the volatile mass efflux, m, are derived for stages (ii), (iii), and (iv), with m = 0 in the first stage. The calculations indicate that during the initial pyrolysis stages (kinetically controlled regime), the surface temperature governs the volatile production rate, whereas during the thick char stage (diffusion-controlled regime), the temperature gradient governs the volatile production rate. Comparisons between the calculated results and numerical computations were made for volatile mass efflux, surface temperature, and density.

Gong et al. [25] initially conducted thermogravimetric analysis (TGA) tests to parameterize the pyrolysis model using the model fitting method. Subsequently, gram-scale autoignition experiments with five power-law heat fluxes (HFs) were performed in a newly designed apparatus. The thermodynamics of oriented strand board (OSB) were determined through inverse modeling, combining an improved numerical model with measured surface temperatures and mass loss rates under a moderate HF. The model's extrapolation capability was verified by simulating additional experimental measurements under different heating scenarios. Critical temperature and critical mass flux were utilized to predict autoignition times. The results demonstrate that the developed pyrolysis model accurately captures the measured mass and mass loss rate from the TGA tests. Additionally, there was good agreement between the simulated and measured surface temperatures and mass loss rates in bench-scale tests, despite minor divergences due to observed cracks in the generated char layer. Other authors have also investigated wood degradation phenomena, such as [26–32].

Majdalani et al. [33] developed a simplified compartment fire model to evaluate the fuel contribution of exposed timber elements. The study concluded that the potential for convective fire spread is positively correlated with the percentage of exposed timber surface area. When exposed to fire, load-bearing mass timber structures, such as cross-laminated timber (CLT), soften and decompose, resulting in significant deformation and weakening, which ultimately leads to structural failure. A combined experimental and modeling analysis is presented to predict the post-fire residual compression properties of CLT. Multiple experimental fire exposure and post-fire mechanical tests were conducted by Loh & Barnett [34] under identical conditions to characterize the internal and external thermal responses of the CLT and evaluate its residual compression properties. An analytical modeling strategy, based on the measured through-the-

thickness temperature profile during fire exposure, is introduced to predict the residual compression properties. X-ray computed tomography analysis revealed a nonconstant charring rate, consistent with current research findings but not with Eurocode design suggestions. The analytical analysis indicated that the transverse (cross) laminae contribute minimally to the axial compression properties but play a critical role in providing thermal protection and maintaining the structural integrity of the longitudinal (load-aligned) laminae during fire exposure.

Khelifa et al. [35] investigated a study to propose a model that accounts for the variation of thermophysical properties, the development of char, and its evolution with temperature. This model integrates a sequential coupling of heat transfer analysis with structural response. The degradation of material properties is considered using the regulatory approach recommended in Eurocode 5. Stress analysis employs an elasto-plastic model with nonlinear isotropic hardening. The model is implemented within the Abaqus finite element software using external subroutines. Its predictions align well with experimental data, accurately reproducing both thermal and structural responses. Specifically, the model accurately predicts temperature profiles, displacements, and the depth of the charred layer, which begins to form above 300 °C.

The behavior of Algerian white wood (AWW) under high temperatures has been rarely considered in the current available literature. This study addresses this significant gap by investigating the phenomena resulting from a fire and determining key properties: the loss of mass and temperature evolution, which are crucial factors for the mechanical behavior of white wood when exposed to fire. Understanding these properties is essential for its application in construction, particularly in Algeria where it is used in individual houses and as structural elements in roof frameworks. By providing new insights into the fire behavior of white wood, this research contributes to safer and more sustainable construction practices, promoting the use of this environmentally friendly material in the building industry.

To analyze the behavior of AWW under various high-temperature conditions, we conducted an experimental study on wooden specimens with dimensions of 8×8×32 cm. The samples were heated in electric ovens at four different temperature levels (150 °C, 200 °C, 300 °C, and 400 °C) for one hour. The physical and mechanical properties of wood at ambient temperature were previously determined through experimental work. Additionally, we performed a numerical study using the SAFIR [36] code on the same type of samples. This approach offers a fairly good understanding of the high temperature behaviour of AWW.

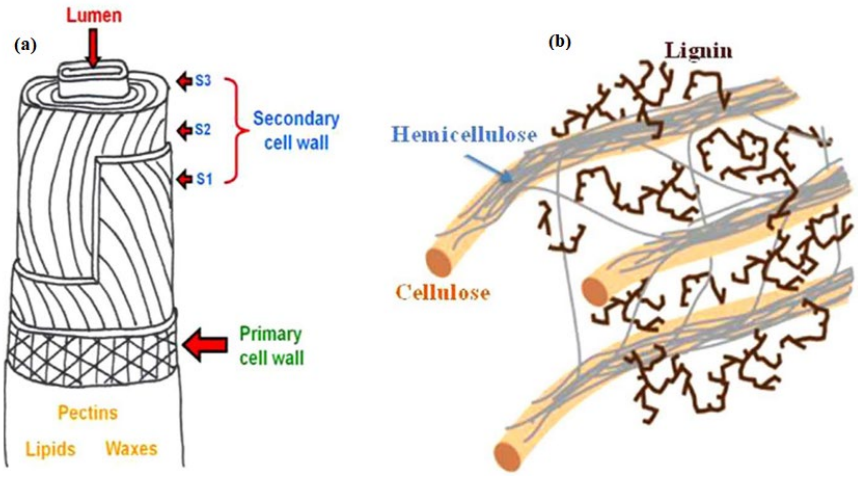

Figure 1. (a) Cell wall structural organization. (b) Cell wall polymer interactions in secondary cell wall of hardwood [6].

2. Materials and Methods

2.1. Materials

This study utilized a commercially prevalent Algerian softwood (AWW), locally known as 'white wood', selected for its direct relevance to regional construction practices. Although a precise botanical classification was unavailable, the timber is characterized as a low-density, light-colored softwood with properties comparable to European spruce (*Picea abies*). This is supported by an average air-dry density of 507.25 kg/m^3, moisture content of 15.35 % and mechanical properties – including a tangent modulus of ≈1779 MPa, tensile strength of ≈100 MPa, and compressive strength of ≈36 MPa – that fall within the expected range for spruce. Full material characterization is provided to guarantee the reproducibility of the experimental work.

2.2. Experimental Study

This study subjected specimens to four heating-cooling cycles from an ambient temperature of 30 °C to target temperatures of 150 °C, 200 °C, 300 °C, and 400 °C in an electric oven (Fig. 2). A heating rate of 12 °C/min was used to simulate severe fire conditions approximating the standard ISO 834 fire curve. The specimens were positioned to ensure even heat distribution. For the 200 °C and 300 °C cycles, a thermocouple placed near the center of the sample sections (Fig. 2b) recorded temperatures at five-minute intervals. As illustrated in Fig. 3 and consistent with the literature [15], the effects of heat were reversible for temperatures below 100 °C (Zone 1).

Figure 2. Type of furnace used: (a) specimen in 300 °C heating, (b) furnace containing a sample with a thermocouple.

Furthermore, prolonged exposure to temperatures exceeding 65 °C leads to persistent alterations in the wood mechanical characteristics. As the temperature approaches 100 °C, the wood rapidly loses its free water, followed by its bound water. The temperature plateaus until all the water has completely evaporated. A rapid temperature increase then results in a slow loss of solid mass up to approximately 240 °C due to pyrolysis (Zone 2). At temperatures around 300 °C (Zone 3), the pyrolysis process releases flammable gases, and the wood is considered carbonized. Consequently, charring layers form and advance through thermal conduction within the material. The combustion of wood, which begins between 150 °C and 200 °C, releases gases including non-combustible carbon dioxide and combustible carbon monoxide [16–18].

2.3. Numerical Study: Thermal and Mechanical Analysis

The numerical study considered the following thermal properties: thermal conductivity, specific heat capacity, density, and emissivity. The convection coefficient ($W/m^2 \cdot K$) and emissivity (–) for both heated and unheated surfaces were also defined. According to Eurocode EN 1991-1-2, the recommended convection coefficient for heated surfaces is 25 $W/m^2 \cdot K$ under standard time–temperature curves, while for unheated surfaces, a value of 4 $W/m^2 \cdot K$ is suggested when radiation heat transfer effects are not taken into account. The recommended emissivity, unless otherwise specified in the material-related fire design parts of the Eurocodes, is 0.8.

The mechanical properties of this type of wood (AWW), determined from previous experiments under normal conditions, are as follows on: tangent modulus = 1779 MPa, tensile strength = 100 MPa, and compressive strength = 36 MPa.

According to Annex B of EN 1995-1-2:2004 [7] for 'WOODEC5', the thermal behavior of wood is considered purely conductive, using modified thermal properties that represent complex phenomena. Two-dimensional numerical models of wood sections were developed in SAFIR, with the grain direction oriented perpendicular to the section.

3. Results and Discussions

3.1. Experimental Results

3.1.1. State of specimens after heating

Table 1. Mass loss of wood specimens.

N°	Level of temperature	Mass before heating (g)	Mass after heating (g)	Mass loss (%)
1	150°C	935	917	1.93
2	200°C	933	850	8.89
3	300°C	984	502	48.98
4	400°C	1034	409	60.44

The mass of the test specimens was measured before and after each heating cycle, revealing a consistent decrease in mass with increasing temperature. The calculated mass loss for each cycle is presented in Table 1.

At 150 °C, the mass loss was negligible (approximately 2 %) and was accompanied by a color change from white to red, indicating the evaporation of free and bound water. As the temperature increased to 200 °C, the mass loss became more substantial, rising to 9 %.

Significant mass loss occurred at 300 °C and 400 °C, exceeding 50 % of the original mass (Fig. 3), a finding consistent with prior studies [23, 24]. These high-temperature cycles were also characterized by copious smoke emission (Figs. 4 and 5), a strong odor, and the blackening of wood due to carbonization.

Furthermore, the adhesive bond between the wood components deteriorated, leading to detachment. This is attributed to the thermal degradation of the glue. The pyrolysis process at these temperatures (200 °C and above) released combustible gases, including carbon monoxide (CO) and carbon dioxide (CO_2), with CO concentration increasing significantly in the high-temperature zone (above 300 °C) [25, 26]. While wood typically contains minimal nitrogen and sulfur, its behavior shares similarities with other biomass materials like coal, though wood generally has a lower aromatic content.

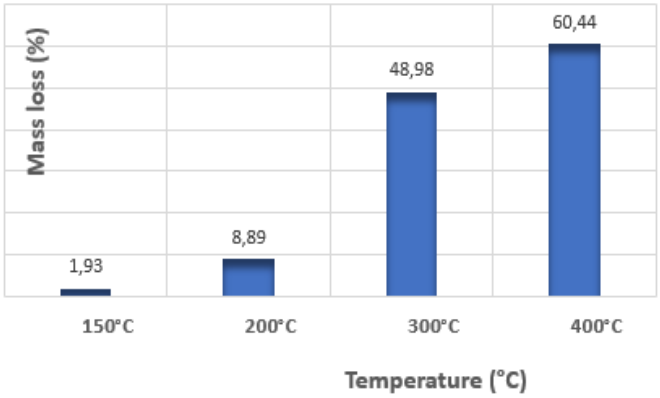

Figure 3. Mass loss of used specimens.

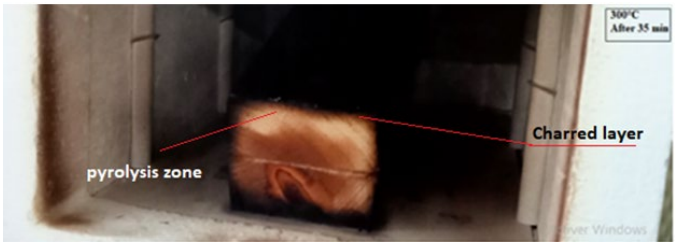

Figure 4. Specimen exposed at 300 °C.

Figure 5. Specimens after exposition to different heating rates, during 60 min.

Fig. 4 shows the cross-section of wood exposed to 300 °C. Different parts are identified: a charred layer, a layer of pyrolysis (about 5 mm) and the core of the intact section.

Smoke emission was observed from 200 °C during the heating phases, indicating the release of volatile gases, including CO and CO_2. This marks the onset of pyrolysis, where wood decomposes into char, non-flammable gases (e.g. water vapour, CO_2), and combustible gases (e.g. CO, H_2, hydrocarbons).

The concentration of combustible gases, particularly CO, increases with temperature [15–18]. The exothermic combustion of these released gases further elevates the system temperature.

When the temperature reached 400 °C, a distinct shift occurred towards dominant char production at the expense of volatile gas release (Zone 4). At this stage, the specimen was cooled outside the oven (Fig. 5).

This thermal degradation behavior is governed by the decomposition of wood primary constituents. Hemicellulose decomposes first (200–260 °C), producing acetic acid. Cellulose degrades between 240–350 °C, forming levoglucosan, while lignin decomposes over a broad range (280–500 °C) and is the primary contributor to char formation [17].

3.1.2. Temperature variation in the cross-section

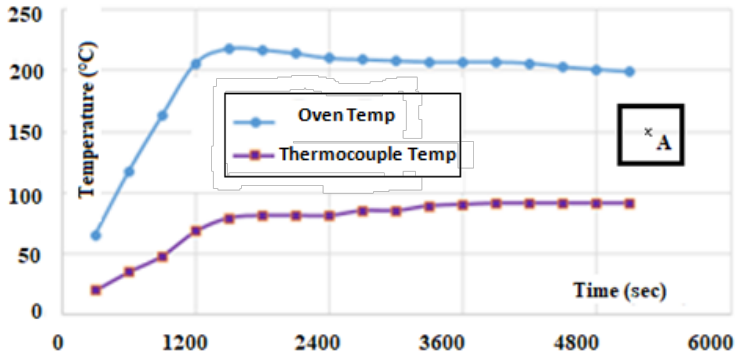

Figure 6. Temperature variation at point in central zone for hating level of 200 °C.

Fig. 6 displays the temperature profiles over time for the furnace air and the center of the wood specimen. The oven temperature rose over 20 min before stabilizing at the target of 200 °C. The temperature at the wood center followed a similar trend in both the 200 °C and 300 °C tests (Fig. 7), consistent with references [19, 20]. However, the wood heated more slowly, creating a thermal lag and a sustained ~100 °C difference from the oven temperature.

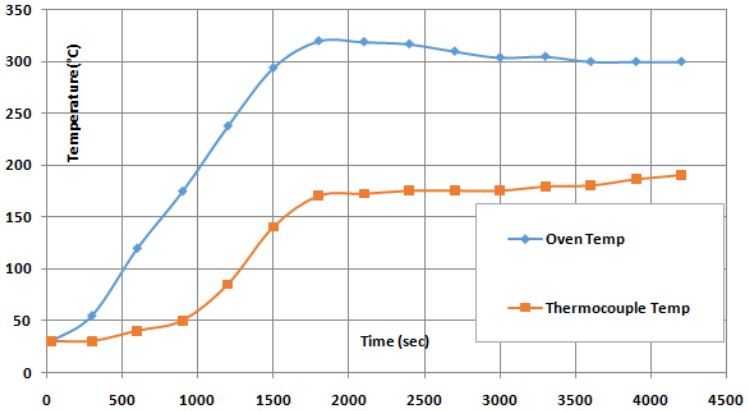

Figure 7. Temperature variation at point in central zone for hating level of 300 °C.

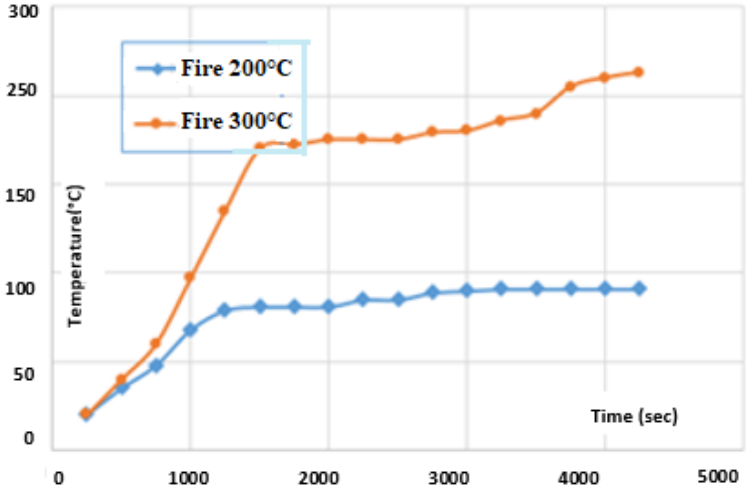

Figure 8. Temperature variation at point in central zone for hating level of 200 °C and 300 °C.

According to Fig. 8, the temperature evolution at a point in the central zone can be observed. At the 200 °C heating level, the temperature curve initially increases with time and then stabilizes at values not exceeding 100 °C. In contrast, at the 300 °C heating level, the temperature at the considered point rises rapidly to approximately 175 °C, remains stable for about 30 min, and then increases again, reaching around 225 °C at the end of the test. This marks the onset of thermal degradation for this type of wood.

It was also observed that during oven cooling (as the furnace temperature decreased to 30 °C), the temperature at the center of the specimen continued to rise, reaching about 270 °C after one hour. After several hours of cooling, the entire sample turned black, indicating significant polymerization of cellulose, which typically occurs in the 300–350 °C range. Chemical reactions occurring at this stage are consistent with findings reported in the literature [21–24].

This study demonstrates that the energy balance at the combustion surface is mainly influenced by the intensity of the heating conditions, which directly affect the evolution of wood mechanical properties [29, 30] (see Fig. 5). These aspects will be analyzed in the future work.

3.2. Numerical Results

3.2.1. Temperature variation in the cross-section

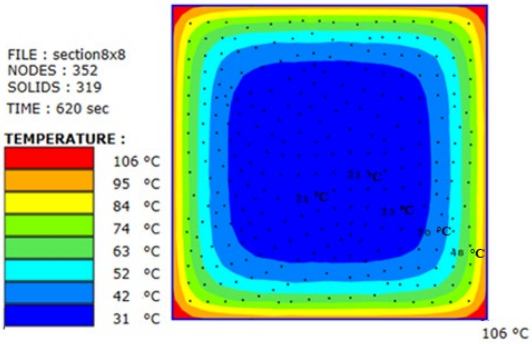

Figure 9. Temperatures distribution within the wood section, considering the heating curve of the furnace during 620 sec (10 min).

Based on the thermal analysis results, the central zone reached a temperature of 21 °C after 10 min of fire exposure (Fig. 9). Moving away from the central zone, the temperature increased; at the corner, it reached 106 °C after 10 min, corresponding to the onset of water evaporation. After 60 min (1 hour), the temperature at this location rose to 299 °C (Fig. 10), which is approximately equal to the furnace temperature corresponding to the 300 °C heating level.

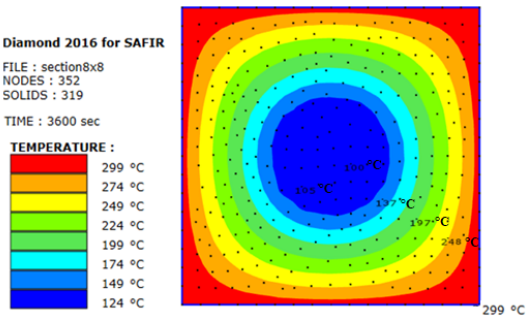

Figure 10. Temperatures distribution within the wood section, considering the heating curve of the furnace during 3600 sec (60 min).

According to Fig. 10, during 60 min of exposure in the furnace, the central zone of the wood section reached a temperature of approximately 100 °C (blue area), corresponding to the release of moisture. The intermediate zone exhibited temperatures in the range of 100–200 °C (light blue and green areas), indicating the onset of the pyrolysis process. Finally, the outermost region, referred to as the charred zone, was represented by yellow, brown, and red colors. The temperature variations at three points within these defined zones are illustrated in Fig. 11.

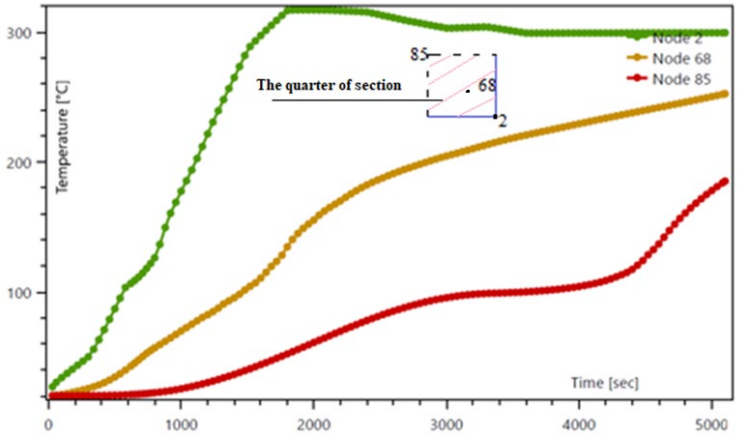

Figure 11. Temperature at the nodes 85, 68, and 2 in the section column heated in the furnace.

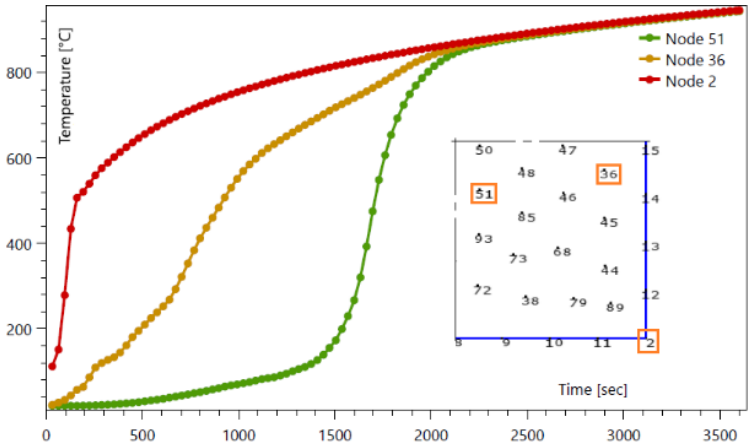

Figure 12. Temperature at the nodes 51, 36, and 2 in the column section exposed to ISO834 fire.

The graphs in Fig. 12 show the temperature variation at three locations on a wood section exposed to the standardized ISO834 fire. Node 2 is at the section corner, and its temperature curve closely follows the ISO834 fire curve. Node 36 is located on the edge of the section, and Node 51 is at the center.

It is clear that the temperature at Node 36 increases more rapidly than at the central Node 51. The standard fire is more severe than the oven fire used in previous tests, which explains why the temperature at the center of the section (Node 51) reaches 900 °C after 60 min in this scenario. These results are in accordance with [19–21].

Fig. 13 shows the progression of carbonization in the section after 25 min of fire exposure. In the normalized fire (Fig. 13a), the charred layer (represented in red) is significant at this stage, a finding

consistent with [19]. Green represents the pyrolysis zone (degrading wood), while blue represents the wood that has lost all its water (dry wood).

As shown in Fig. 13b, the central area (blue) remains quite wide, with a maximum temperature of 55 °C, indicating the fire has not yet reached this wood. Thermal degradation begins around 200 °C to 250 °C (red part), a threshold that aligns with the experimental findings presented in Fig. 5.

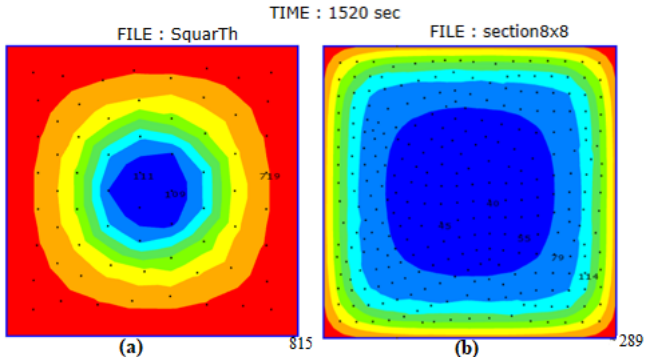

Figure 13. Temperatures distribution within the wood section after 25 min, considering the ISO834 curve fire (a) and heating curve of the furnace (b).

In conclusion, the three distinct zones described in the literature [20–22] – pyrolysis, carbonization, and the core of intact wood – are more clearly observed in the simulation (Fig. 13b) after a 25-minute heating period. This enhanced clarity is due to the specimen's small cross-section, a phenomenon that was also confirmed experimentally (Fig. 4).

According to the model by Khelifa et al. [35], the charred layer begins to form at temperatures above 300 °C. In a rectangular section exposed to fire on all faces, this process causes the residual section to lose its original shape. Furthermore, as the charred layer lacks mechanical strength, the overall load-bearing capacity of the fire-exposed cross-section is reduced [23, 34]. The results of this study are consistent with this model and with the findings of [20, 21].

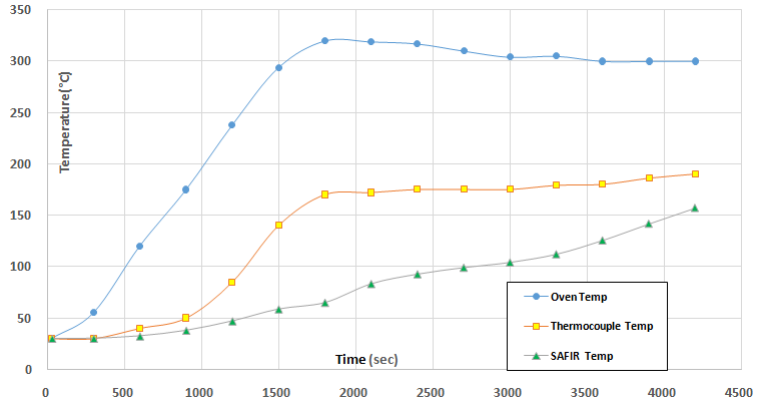

Figure 14. Comparison of numerical and experimental temperature results at a central point, considering a heating level of 300 °C.

Fig. 14 presents two curves illustrating the temperature evolution obtained from the numerical results (blue and brown). The blue curve corresponds to a point located at the corner of the section and closely follows the furnace temperature curve with a heating level of 300 °C. The second curve represents a point at the center of the section. A third curve (gray and green), also corresponding to this central point, is derived from the experimental results. The curves showing the temperature evolution in the central zone display a noticeable deviation. It is important to note that the experimental curve exhibits a rapid increase between 1000 sec and 1750 sec, which can be attributed to the relatively high heating rate applied in this study (12 °C/min).

3.2.2. Residual tangent modulus

At the beginning of heating (30 sec), a slight variation in the tangent modulus is observed, particularly at the corners and along the edges of the element. It can be seen that the tangent modulus of wood decreases due to the rise in temperature (Fig. 15). After 742 sec – the failure time of the wood element – the tangent modulus has significantly decreased. At the upper corners, it reaches a value of zero, while along the edges it is approximately 660 MPa. This value increases toward the center of the section, ranging between 880 MPa and 1540 MPa (Fig. 16).

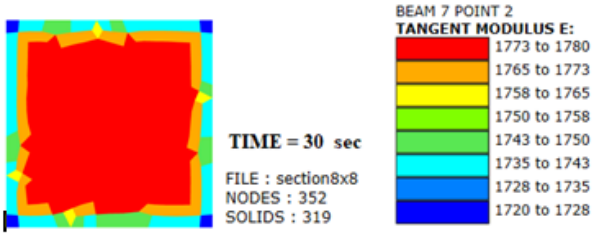

Figure 15. Residual tangent modulus at 30 sec.

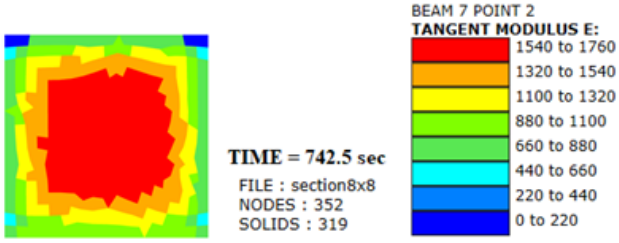

Figure 16. Residual tangent modulus at failed time (742.5 sec).

In SAFIR, the elements of the section considered in the thermal analysis are modeled as fibers when coupling heat transfer with structural behavior. Each fiber possesses mechanical properties that evolve with temperature over time. Fig. 17 presents four curves, each corresponding to a specific fiber within the structural element.

The selected fibers provide insight into the behavior of different regions: the central zone (Fib 117), the edges (Fib 69), and the corners (Fib 205 and Fib 208). The corner and edge fibers generally exhibit similar behavior – their curves decrease over time, indicating a reduction in the tangent modulus to about 600 MPa, approaching failure at approximately 675 sec. For the top-corner fiber (Fib 208), a rapid drop to zero is observed. Fiber 205 initially shows an increase followed by stabilization around 900 MPa, which can be attributed to the anisotropic nature of wood. The edge fiber (Fib 69) also exhibits a decrease in tangent modulus with time and increasing temperature but maintains a difference of about 300 MPa compared to the corner fibers, reaching 700 MPa at failure. In contrast, the central-zone fiber (Fib 117) shows no variation in its tangent modulus.

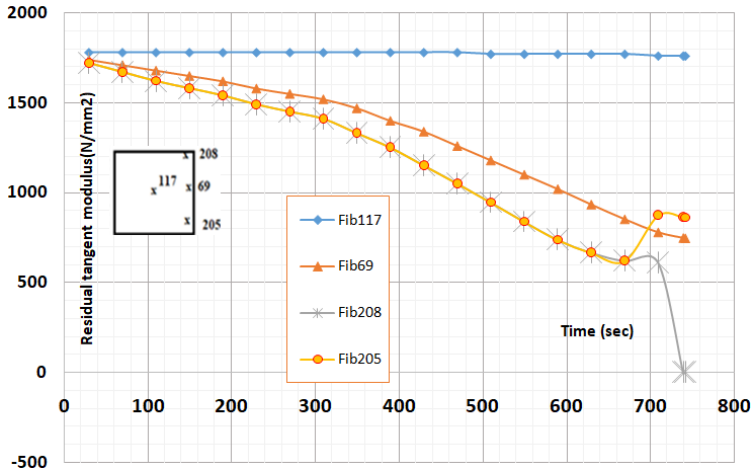

Figure 17. Residual tangent modulus evolution according the time.

This observation is consistent with expectations, as during this period (700 sec), the temperature in this zone remains below 50 °C, as indicated by both the numerical and experimental curves (Fig. 14). Accordingly, the wood in this region retains its integrity and exhibits no signs of thermal degradation.

4. Conclusion

The results of this work lead to the central conclusion that the vulnerability of AWW in fire scenarios stems not only from the degradation of the wood itself but also from the premature failure of its glued connections.

1. This experimental and numerical study delineates the thermal degradation process of wood, revealing a clear sequence of moisture loss, pyrolysis, and charring. The mass loss was negligible at 200 °C but became substantial (exceeding 50 %) at temperatures of 300 °C and above, accompanied by significant smoke and the release of CO and CO_2. A critical finding was the mechanical failure of glued sections at these higher temperatures, highlighting vulnerability in constructed elements. Furthermore, the analysis of individual fibers provided a novel, micromechanical perspective, demonstrating a progressive weakening at the edges and corners while the core remained stable and intact.

2. A key scientific contribution of this work is the successful validation of a thermo-mechanical model using SAFIR software. The simulation results demonstrated a close alignment with experimental data, accurately capturing phenomena such as char layer formation and the preservation of an intact core after a 25-minute heating period. This validates the model as a reliable tool for predicting the behavior of timber sections under fire conditions, which can reduce the reliance on costly and time-consuming experimental testing.

3. Our findings both confirm and supplement prior research. The observed stages of degradation – free and bound water loss followed by pyrolysis and carbonization – are consistent with the established literature on wood combustion [26–32]. Similarly, the formation of a protective char layer and the survival of a cool, intact core align with classical theories of timber fire performance. However, this study supplements this knowledge by quantitatively linking these thermal phenomena to the localized mechanical degradation, specifically the time-and temperature-dependent reduction of the tangent modulus in peripheral fibers. The observed adhesive failure at 300 °C also presents a critical, practical finding that may not be fully accounted for in models focusing solely on solid timber.

5. Implications and Future Work

In conclusion, this research provides a validated framework for analyzing the fire-induced mechanical degradation of wood, with specific insights into the behavior of AWW (cf. *Picea abies*). The demonstrated sensitivity of this timber to the heating source's magnitude and properties underscores the need for material-specific characterization. The central objective of subsequent studies will be to map the progression of residual mechanical properties, thereby refining predictive models to enable safer timber structural design.

References

1. National Lumber Manufacturers Association. Wood Structural Design Data. Vol. 1. 2nd ed. Washington, 1941. 296 p.
2. Hansen, H.J. Timber Engineers Handbook. John Wiley & Sons. New York, 1948. 882 p.
3. CEN. Eurocode 5: Design of timber structures. Part 1-2: General – Structural fire design. EN 1995-1-2. European Committee for Standardization. Brussels, 2004. 71 p.
4. Schweingruber, F.H. Wood Structure and Environment. Springer. Berlin, Heidelberg, 2007. XII + 279 p. DOI: 10.1007/978-3-540-48548-3.
5. Dinwoodie, J.M. Timber: its nature and behaviour. 2nd ed. Taylor and Francis. Abingdon, United Kingdom, 2000. 257 p.
6. Ramage, M.H., Burridge, H., Busse-Wicher, M. The wood from the trees: The use of timber in construction. Renewable and Sustainable Energy Reviews. 2017. 68(1). Pp. 333–359. DOI: 10.1016/j.rser.2016.09.107
7. Cotton, C.M. Ethnobotany: Principles and Applications. John Wiley and Sons. Chichester, 1996. IX + 424 p.
8. Hillis, W.E. Heart Wood and Tree Exudates. Springer. Berlin, Heidelberg, 1987. XIV + 268 p. DOI: 10.1007/978-3-642-72534-0
9. The American Wood Council (AWC). Wood Structural Design Data. 1986 Edition with 1992 Revisions. American Forest & Paper Association. Washington, 2004. 270 p.
10. Švajlenka, J., Pošiváková, T. Innovation potential of wood constructions in the context of sustainability and efficiency of the construction industry. Journal of Cleaner Production. 2023. 411. Article no. 137209. DOI: 10.1016/j.jclepro.2023.137209
11. Budykina, T.A., Anosova, Ye.B. Thermal resistance of fire retardant materials. Magazine of Civil Engineering. 2022. 112(4). Article no. 11213. DOI: 10.34910/MCE.112.13
12. Tsvetkov, N.A., Tolstykh, A.V., Khutornoi, A.N., Boldyryev, S., Kolesnikova, A.V., Tsvetkov, D.N. Thermophysical analysis of heat-insulated glued laminated profiled timber for wooden houses. IOP Conference Series: Earth and Environmental Science. 2021. 866. Article no. 012037. DOI: 10.1088/1755-1315/866/1/012037
13. Zhou, T., Liu, H. Research Progress of Wood Cell Wall Modification and Functional Improvement: A Review. Materials. 2022. 15(4). Article no. 1598. DOI: 10.3390/ma15041598
14. Purkiss, J. Fire Safety Engineering: Design of Structures. 2nd ed. CRC Press. London, 2006. 424 p. DOI: 10.1201/b12845
15. Hu, H., Qi, Zh., Shi, J., Li, H., Ji, J. Experimental and numerical investigations on fire development in a timber-based compartment with identification of characteristic events. Journal of Building Engineering. 2024. 87. Article no. 109033. DOI: 10.1016/j.jobe.2024.109033
16. Buchanan, A.H. Fire performance of timber construction. Progress in Structural Engineering and Materials. 2000. 2(3). Pp. 278–289. DOI: 10.1002/1528-2716(200007/09)2:3<278::AID-PSE33>3.0.CO;2-P
17. Dietenberger, M. Update for combustion properties of wood components. Fire and Materials. 2002. 26(6). Pp. 255–267. DOI: 10.1002/fam.807

18. Fawaz, M., Gollner, M.J., Bond, T.C. A novel representation of time-resolved particle emissions from pyrolyzing wood. Biomass and Bioenergy. 2024. 183. Article no. 107054. DOI: 10.1016/j.biombioe.2024.107054
19. Park, W.C., Atreya, A., Baum, H.R. Experimental and theoretical investigation of heat and mass transfer processes during wood pyrolysis. Combustion and Flame. 2010. 157(3). Pp. 481–494. DOI: 10.1016/j.combustflame.2009.10.006
20. Gernay, Th., Zehfuß, J., Franssen, J.-M., Robert, F., Brunkhorst, S., Felicetti, R., Bamonte, P., Mohaine, S., McNamee, R. Experimental assessment of the burnout resistance of timber and concrete columns. SiF 2022 – The 12th International Conference on Structure in Fire. The Hong Kong Polytechnic University. Hong Kong, 2022.
21. Renard, S., Robert, F., Franssen, J-M., Zehfuß, J., McNamee, R., Bamonte, P., Gernay, Th. Structural behavior of timber columns in wood crib compartment fire tests. Fire Safety Journal. 2025. 155. Article no. 104413. DOI: 10.1016/j.firesaf.2025.104413
22. Elshayeb, M., Ab Malik, A.R., Ideris, F., Hari, Z., Ab Razak, N., Siang, J.E.L., Anuar Z., Utilization of Numerical Techniques to Predict the Thermal Behavior of Wood Column Subjected to Fire. Part A: Using Finite Element Methods to Develop Mathematical Model for Wood Column. Key Engineering Materials. 2006. 306–308. Pp. 577–582. DOI: 10.4028/www.scientific.net/KEM.306-308.577
23. Šulc, S., Šmilauer, V., Wald, F. Thermal Model for Timber Fire Exposure with Moving Boundary. Materials. 2021. 14(3). Article no. 574. DOI: 10.3390/ma14030574
24. Wichman, I.S., Atreya, A. A simplified model for the pyrolysis of charring materials. Combustion and Flame. 1987. 68(3). Pp. 231–247. DOI: 10.1016/0010-2180(87)90002-2
25. Castagna, A., Geng, Y., Rein, G. Historical investigation into the first burning model of a solid fuel and the origin of the Crank–Nicolson numerical method. Applications in Energy and Combustion Science. 2025. 24. Article no. 100404. DOI: 10.1016/j.jaecs.2025.100404
26. Zhang, Y., Lu, J., Yu, J., Wang, W., Zhai, Sh., Yu, Yi., Qi, D. A controllable and fast carbonization strategy under air conditions and its application in electromagnetic interference (EMI) shielding. Composites Part A: Applied Science and Manufacturing. 2025. 192. Article no. 108764. DOI: 10.1016/j.compositesa.2025.108764
27. Gong, J., Zhang, M. Pyrolysis and autoignition behaviors of oriented strand board under power-law radiation. Renewable Energy. 2022. 182. Pp. 946–957. DOI: 10.1016/j.renene.2021.11.032
28. Spearpoint, M.J., Quintiere, J.G. Predicting the burning of wood using an integral model. Combustion and Flame. 2000. 123(3). Pp. 308–325. DOI: 10.1016/S0010-2180(00)00162-0
29. Agarwal, P.K. Transport phenomena in multi-particle systems-IV. Heat transfer to a large freely moving particle in gas fluidized bed of smaller particles. Chemical Engineering Science. 1991. 46(4). Pp. 1115–1127. DOI: 10.1016/0009-2509(91)85104-6
30. Yao, X., Yu, Q. Kinetic and experimental characterizations of biomass pyrolysis in granulated blast furnace slag. International Journal of Hydrogen Energy. 2018. 43(19). Pp. 9246–9253. DOI: 10.1016/j.ijhydene.2018.03.173
31. Di Blasi, C. Modeling chemical and physical processes of wood and biomass pyrolysis. Progress in Energy and Combustion Science. 2008. 34. Pp. 47–90.
32. Colombiano, J., Batiot, B., Dréan, V., Richard, F., Guillaume, E., Rogaume, T. Numerical analysis of the characteristics of the decomposition zone of a burning wood sample under cone calorimeter and evaluation of the limiting process. Journal of Analytical and Applied Pyrolysis. 2022. 168. Article no. 105752.
33. Majdalani, A.H., Calderón, I., Jahn, W., Torero, J.L. Understanding Compartmentation Failure for High-Rise Timber Buildings. Fire. 2024. 7. Article no. 190. DOI: 10.3390/fire7060190
34. Loh, T.W., Barnett, J.R. Fire-induced damage and postfire analysis of the compression properties of cross-laminated timber. Journal of Materials in Civil Engineering. 2024. 36(31). Article no. 04023595. DOI: 10.1061/JMCEE7.MTENG-16285
35. Khelifa, M., Thi, V., Oudjène, M., Khennane, A. Modelling the Response of Timber Beams Under Fire. International Journal of Civil Engineering. 2024. 22. Pp. 1537–1549. DOI: 10.1007/s40999-024-00973-2
36. Franssen, J.-M., Gernay, T. User's Manual for SAFIR (Version 2022) – A Computer Program for Analysis Of Structures Subjected to Fire. Part 5: Material Properties. Liege: University of Liege, 2022.
37. Boudjadja, M., Otmani-Benmehidi, N. Thermomechanical behavior of wooden and steel columns in fire situation. ICCEE2023 – 1st International Conference on Civil and Earthquake Engineering. EDP Sciences. Annaba, 2023.
38. Gravit, M.V., Dmitriev, I.I. Numerical modeling of basalt roll fire-protection for light steel thin-walled structures. Magazine of Civil Engineering. 2022. 112(4). Article no. 11215. DOI: 10.34910/MCE.112.15

Information about the authors:

Nadia Otmani-Benmehidi,
ORCID: https://orcid.org/0000-0002-3565-5942
E-mail: nadia.otmani@univ-annaba.dz

Marwa Boudjadja,
ORCID: https://orcid.org/0009-0000-9772-1194
E-mail: marwa.boudjadja@univ-annaba.dz

Abdessalem Otmani,
ORCID: https://orcid.org/0000-0001-8316-1843
E-mail: a.otmani@ensti-annaba.dz

Received 05.07.2024. Approved after reviewing 17.10.2025. Accepted 18.10.2025.